Measurement and Modeling of U(IV) Adsorption to Metal Oxide Minerals

Zimeng Wang,[*,†] Kai-Uwe Ulrich,[‡] Chao Pan,[§] and Daniel E. Giammar[§]

[†]Department of Civil and Environmental Engineering, Stanford University, Stanford, California 94305, United States

[‡]BGD Soil and Groundwater Laboratory, 01219 Dresden, Germany

[§]Department of Energy, Environmental and Chemical Engineering, Washington University in St. Louis, St. Louis, Missouri 63130, United States

S *Supporting Information*

ABSTRACT: Chemical or biological reduction of U(VI) produces a variety of poorly soluble U(IV) species. In addition to uraninite (UO_2) and biomass-associated noncrystalline U(IV), recent research has found adsorbed U(IV) species on mineral surfaces. To build on these observations, we evaluated equilibrium adsorption of U(IV) to magnetite and rutile as a function of pH and total U(IV) loading. Surface complexation models that could successfully simulate the uptake of U(IV) by accounting for UO_2 precipitation and adsorption of U(IV) to both the minerals and the reactor surfaces were developed. Application of the models could determine the conditions under which adsorption as opposed to precipitation would dominate U(IV) uptake with solids. The model-predicted U(IV) surface coverages of the minerals were consistent with a recent spectroscopic study. Such models advance our ability to predict the equilibrium speciation of U(IV) in the subsurface.
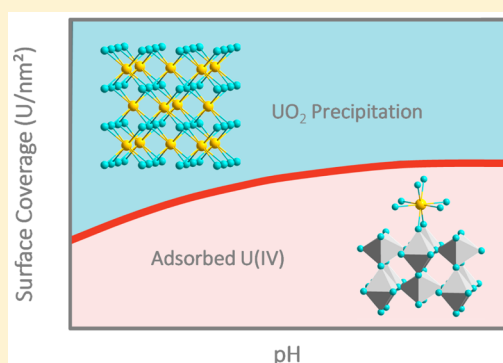
INTRODUCTION

Uranium contamination of subsurface environments is a legacy of past activities of nuclear weapons development and is a continuing concern associated with mining and processing of materials for nuclear energy. Mechanistic knowledge of uranium biogeochemistry is necessary for remediation of contaminated sites and long-term stewardship of geologic repositories. Dominating under oxic conditions, U(VI) is highly soluble and mobile in groundwater. Reduction of U(VI) to U(IV) significantly decreases uranium solubility, which offers the possibility for in situ remediation of uranium in subsurface environments.[1] Solids with structural or surface-associated Fe(II)[2−4] and sulfide[5] are effective abiotic reductants. Reduction of uranium can also be microbially mediated[6,7] or even be mediated by coupled biotic and abiotic pathways.[8] While early research hypothesized that uraninite (UO_2) was the primary U(IV) product,[9−11] noncrystalline U(IV) species were more recently found as additional products of microbial reduction.[12−17] These species are more susceptible to remobilization from a remediated system if they are challenged by complexants or oxidants.[18,19]

Most research on noncrystalline U(IV) has focused on complexation with phosphorus ligands in biomass following biotic reduction,[8,13,20,21] and less attention has been paid to the U(IV) species generated abiotically, particularly those involving mineral surfaces. Boyanov et al. reported that phosphate induced the formation of phosphate-complexed noncrystalline U(IV) from U(VI) reduction by 9,10-anthrahydroquinone 2,6-disulfonate.[17] Chakraborty et al. hypothesized that adsorbed U(IV) was produced from reduction of U(VI) by montmorillonite with adsorbed Fe(II)[22] because no evidence of U(IV) precipitates was found. A recent spectroscopic study by Latta et al. suggested that reduction of U(VI) by a Ti-substituted magnetite produced noncrystalline U(IV) with a molecular-scale structure resembling a U(IV) surface complex with a novel U−Ti binding geometry.[23] They then reported that mineral surfaces can stabilize U as adsorbed U(IV) following U(VI) reduction.[24] As long as the surface loading is sufficiently low, inner-sphere U(IV) surface complexes can persist for several months or longer without transforming to crystalline products.

While these recent discoveries of U(IV) adsorbed to minerals have expanded the family of noncrystalline U(IV) species from reduction-based remediation systems, the lack of understanding of their structure and stability limited our ability to include them in reaction-based frameworks for predicting equilibrium speciation. Consequently, the objectives of our study were (1) to quantify the adsorption equilibrium between aqueous U(IV) and mineral surfaces that are relevant to subsurface environments and (2) to incorporate adsorption reactions into a thermodynamic framework to predict equilibrium U(IV)

speciation in the presence of mineral surfaces. Measurement and modeling of U(IV) adsorption to minerals can lead to an improved understanding of the fate of uranium in the subsurface and the development of more sustainable remediation strategies.

■ MATERIALS AND METHODS

Aqueous U(IV) Solution and Minerals. Our study probed the adsorption equilibrium by reacting aqueous U(IV) with minerals, which is a well-established approach for adsorption studies that is more direct than that of obtaining adsorbed U(IV) by reducing U(VI) at mineral surfaces as was done in previous studies.[22−24] Briefly, aqueous U(IV) was prepared by dissolving synthetic UO_2 in 10 M HCl (Figure S1 of the Supporting Information). Magnetite and rutile were selected as the model geochemical sorbents. Those two minerals are expected to persist under anaerobic conditions stimulated by organic electron donors, and they were previously reported to adsorb U(IV) as surface complexes.[24] We also conducted the experiments with hematite. Further details about the U(IV) solution and minerals are in the Supporting Information. Strict anoxic environments were maintained. A fundamental assumption of our approach was that U(IV) would not be oxidized by the minerals during our experiments. Rutile itself is not expected to act as an oxidant for U(IV) in the dark system. In the uranium geochemistry literature, magnetite has been regarded as an abiotic reductant. Reduction of U(VI) to U(IV) by magnetite has been reported in a number studies at circumneutral pH[25−28] and in a few studies involving low-pH conditions.[29,30] Nevertheless, the Fe(III) in magnetite might serve as an electron acceptor. Thermodynamic calculation indicated that reduction of U(VI) by magnetite at the concentrations used in our experiment was favorable. Therefore, no U(VI) would be anticipated for our system that started with pure U(IV). The oxidation state of U adsorbed to the magnetite was also probed in an extraction test using carbonate;[31] because carbonate forms strong complexes with U(VI) but not with U(IV), it can selectively extract U(VI). For magnetite, this test extracted a negligible amount of uranium, indicating that only U(IV) was adsorbed (details in the Supporting Information).

Batch Experiments. Given that both adsorption and precipitation of cationic metals such as U(IV) become more favorable in going from acidic to neutral pH, the pH dependence of adsorption was evaluated by incrementally increasing the pH from acidic values (2 or 3) with sufficient equilibration time (2 h as confirmed in preliminary kinetic experiments). The pH measured after the equilibration period was recorded as the equilibrium pH. Samples (1.8 mL) were collected under vigorous stirring to ensure a constant solid-to-solution ratio. A NaOH solution was then added to increase the pH to the next level, and the reactors were mixed for an additional 2 h before the next sampling. The samples were rapidly filtered through 0.02 μm alumina-based filters (Whatman Anotop25) with the first several drops discarded (details in the Supporting Information). Samples were preserved in 2% HNO_3 and stored in the anaerobic chamber prior to dilution and analyzed by inductively coupled plasma mass spectrometry (ICP-MS, Agilent 7500ce) with a detection limit of 0.01 μg/L.

The difference between the total concentration added and the equilibrium dissolved concentration represents U(IV) uptake. Besides adsorption to minerals, U(IV) loss could be due to UO_2 precipitation and adsorption to the reactor.

Distinguishing adsorption of U(IV) to the reactor from that to minerals and precipitation was allowed by comparing U concentrations in filtered and unfiltered samples (details in the Supporting Information). To obtain the adsorption equilibrium of poorly soluble U(IV), it is critical to perform experiments without interference of precipitation. We selected a total U(IV) concentration of 0.01 μM, which is sufficiently low to maintain undersaturation of UO_2.

Surface Complexation Modeling. With the evidence that U(IV) surface complexes persist for months,[24] adsorption of U(IV) to minerals can be described by surface complexation reactions. The results were simulated using the diffuse double-layer model implemented in MINEQL+.[32] The model contains the surface protonation/deprotonation reactions of the surface hydroxyl groups on the minerals (i.e., ≡FeOH and ≡TiOH), the aqueous speciation reactions of U(IV), the precipitation of UO_2, and the reactions responsible for U(IV) adsorption (Table 1). The specific surface areas of the minerals were

Table 1. Reactions and Equilibrium Constants Considered in the Modeling

equilibrium reaction[a]	log K^{0b}	log $K^{\theta c}$
UO_2 Precipitation		
$U^{4+} + 2H_2O \rightleftharpoons UO_{2(am)} + 4H^+$	−2.61	NA
Reactor ($[\equiv XOH]_{total} = 3 \times 10^{-8}$ M, nonelectrostatic[d])		
$\equiv XOH \rightleftharpoons \equiv XO^- + H^+$	−7.2[e]	NA
$\equiv XOH + U^{4+} + 4H_2O \rightleftharpoons \equiv XOU(OH)_3 + 4H^+$	−1.37	NA
Magnetite ($[\equiv Fe_mOH]_{total} = 5.16 \times 10^{-4}$ M, $A = 67.1$ m²/g)		
$\equiv Fe_mOH + H^+ \rightleftharpoons \equiv Fe_mOH_2^+$	4.7[f]	4.89
$\equiv Fe_mOH \rightleftharpoons \equiv Fe_mO^- + H^+$	−8.09[f]	−7.9
$\equiv Fe_mOH + U^{4+} + 4H_2O \rightleftharpoons \equiv Fe_mOU(OH)_3 + 4H^+$	−4.8	−4.61
Rutile ($[\equiv TiOH]_{total} = 3.13 \times 10^{-5}$ M, $A = 4.1$ m²/g)		
$\equiv TiOH + H^+ \rightleftharpoons \equiv TiOH_2^+$	4.06[g]	3.03
$\equiv TiOH \rightleftharpoons \equiv TiO^- + H^+$	−7.21[g]	−8.23
$\equiv TiOH + U^{4+} + 4H_2O \rightleftharpoons \equiv TiOU(OH)_3 + 4H^+$	−2.21	−3.23
U(IV) Aqueous Reactions (10 mM chloride provides a constant ionic strength)		
$U^{4+} + H_2O \rightleftharpoons U(OH)^{3+} + H^+$	−0.54[h]	NA
$U^{4+} + 2H_2O \rightleftharpoons U(OH)_2^{2+} + 2H^+$	−1.1[h]	NA
$U^{4+} + 3H_2O \rightleftharpoons U(OH)_3^+ + 3H^+$	−4.7[h]	NA
$U^{4+} + 4H_2O \rightleftharpoons U(OH)_{4(aq)} + 4H^+$	−10.0[h]	NA
$U^{4+} + Cl^- \rightleftharpoons UCl^{3+}$	1.72[h]	NA
$U^{4+} + 2Cl^- \rightleftharpoons UCl_2^{2+}$	0.06[h]	NA

[a]The U(IV) surface complexation stoichiometry (i.e., fully protonated neutral species) was found to be the only choice that could simulate the full adsorption edge data with a single reaction. The same stoichiometry was used to model surface complexation reactions of adsorption of other tetravalent metals to minerals at subsurface relevant pH.[50,51] We cannot rule out the existence of other surface complexes (e.g., bidentate[24]), or other combinations of surface reactions that could give equally good or better fits; however, refining the models with a structurally consistent reaction framework was not central to our research objectives. [b]Equilibrium constants as inputs in MINEQL+ corresponding to an ionic strength of zero. The values without references are from this study. [c]Intrinsic equilibrium constants normalized to a standard site density (10 sites/nm²) and a specific surface area (10 m²/g). See conversion equations in refs 34 and 33. [d]For the sake of simplicity and pragmatic considerations, adsorption of U(IV) to the reactor was modeled as a nonelectrostatic reaction. The key to having this reaction in the model was to account for U(IV) loss that was not due to adsorption to minerals or precipitation. [e]Treated as a quartz surface. From ref 47. Employed in ref 43. [f]From ref 48. [g]From ref 49. [h]From ref 38.
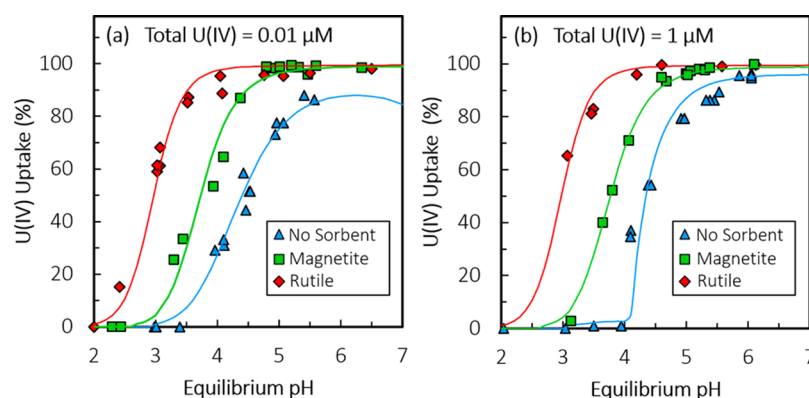
Figure 1. Uptake percentage of U(IV) as a function of pH at total U(IV) concentrations of (a) 0.01 and (b) 1 μM. The solid concentration was 2 g/L. At 0.01 μM total U(IV) in the absence of sorbent, the U(IV) uptake was due to adsorption to the reactor surface. At 1 μM total U(IV) in the absence of sorbent, U(IV) uptake was primarily due to UO_2 precipitation. The lines represent the results of the model simulations. The predicted U(IV) speciation in the presence of sorbents is shown in Figure S2 of the Supporting Information.

incorporated into the model in calculating the total site quantity and surface charge density. Constants for surface reactions from the literature were modified to account for the variations in site density and specific surface area between the materials used in the previous studies and in the work presented here.[33,34] A unique feature of the model was inclusion of adsorption sites on the surface of the reactor, which could have a small but appreciable collection of sites similar or identical to those on quartz.

A site density of 2.3 sites/nm², which was recommended for parsimonious modeling of mineral surface site quantities, was used for all minerals in the study.[35] A fixed value allows a unified comparison framework. The equilibrium constant for adsorption of U(IV) to the reactor was obtained from the mineral-free control experiments with 0.01 μM total U(IV). The mineral-free control experiments with 1 μM total U(IV) were used to explore an applicable log K for UO_2 precipitation. For the U(IV)−mineral reactions, the 0.01 μM U(IV) data were used to obtain the optimal equilibrium constants by minimization of the sum of squares of residuals between the experimental and simulation results. The ability of these constants to simulate U(IV) uptake at a loading of 1 μM was then examined.

RESULTS AND DISCUSSION

Mineral-Free Control Experiments. At 0.01 μM total U(IV), the loss of U was attributed to adsorption to the inner surface of the reactor, which was confirmed by the similar extents ($\pm$10% variation for all pH values) of loss of U from the filtered and unfiltered samples. The significant loss of U(IV) from solution at neutral pH was not surprising given that the total U(IV) concentration was very low.[36,37] The pH dependence of uptake of U(IV) to the reactor could be modeled as an equilibrium reaction (Figure 1a and Table 1). Other combinations of equilibrium constants and site concentrations could provide equally good fits, but the exact combination was not central to our overall objective because our main goal in this part of the modeling was to account for loss of U(IV) from solution that is not due to adsorption to minerals or to UO_2 precipitation (more discussion in the Supporting Information).

With the adsorption equilibrium of U(IV) to the reactor considered in the model, the uptake of U(IV) could then be simulated by optimizing the equilibrium constant for UO_2. At 1

μM total U(IV), the drastic loss of U above pH 4 was attributed primarily to UO_2 precipitation. We note that the log K for UO_2 obtained in this study (-2.61) was lower than the value (-1.5) in a review.[38] Nevertheless, the equilibrium constant obtained here was still within the reasonable range (lower bound of -2.68[39]), especially after considering the particle size and temperature variation (lower bound of 20 °C). At high U(IV) loadings, the model predicted that adsorption to the reactor was negligible due to the supply of surface sites that was orders of magnitude smaller. The log K for UO_2 also predicted that the low-U(IV) experiments were free of precipitation. Once equilibrium constants were established for loss of U(IV) from solution in the absence of minerals, they were used to separate those processes from adsorption to the mineral and UO_2 precipitation.

Adsorption of U(IV) to Minerals. At 0.01 μM total U(IV), where only adsorption to the reactor walls and to the added minerals was involved, the presence of mineral sorbents shifted the adsorption edges to lower pH values; rutile enhanced U uptake the most (Figure 1a). A robust interpretation of the results was allowed by surface complexation modeling in which the interfacial reactions on the mineral surface were incorporated into the existing model for U(IV) uptake in the control experiments. The modeling results (Figure S2 of the Supporting Information) at low U(IV) loadings showed that magnetite was more responsible than the reactor surface for U(IV) adsorption. Rutile was such a strong sorbent for U(IV) that essentially all U(IV) was adsorbed to rutile and none was adsorbed to the reactor. The likely occurrence of some U(IV) oxidation with the hematite had a less straightforward interpretation, so we present the results and discussions in the Supporting Information.

Adsorption versus Precipitation. The presence of mineral surfaces can affect the distribution of U(IV) between adsorbed and precipitated species (Figure 1b). At low pH, the presence of rutile and magnetite induced more U(IV) uptake than in mineral-free control experiments, because of their contribution of sites for adsorption as another pathway for loss of U(IV) from solution.

The surface complexation reactions of the models, which were calibrated using the low-U(IV) data, could also predict the results obtained with high U(IV) loading (Figure 1b). Whereas UO_2 precipitated in mineral-free control solutions in which the pH was >4, the model predicted that no UO_2 would precipitate
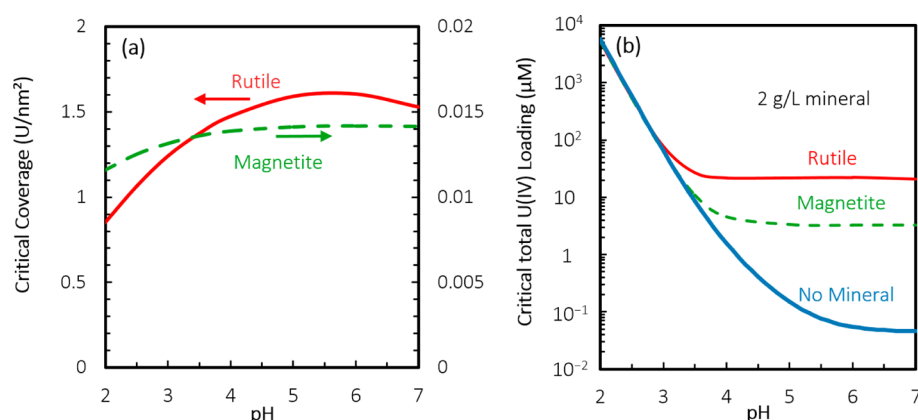
Figure 2. Critical coverages (a) and loadings (b) of U(IV) above which U(IV) would precipitate as UO_2 and below which U(IV) can be stabilized as absorbed U(IV). The simulations were performed by incrementally increasing the total U(IV) concentration until UO_2(s) became supersaturated. If UO_2 was allowed to precipitate in the model, then lines in panel a mean the largest possible surface coverage of U(IV) on these minerals. The critical coverage (a), which is normalized to the mineral surface area, is an intrinsic measurement of the adsorption affinity between U(IV) and the mineral and is independent of the solid and total U(IV) loadings. The critical total U(IV) loading (b) depends on the specific sorbent loading.

when rutile or magnetite was present and that all of the loss of U(IV) from solution could be ascribed to adsorption.

Critical Coverage and Total U(IV) Loading. The preceding results highlight that the stability of U(IV) surface complexes on minerals reported in previous studies[22−24] is due to the more favorable thermodynamics of adsorbed species than of UO_2 over a wide range of water chemistry conditions, especially those with lower pH values and lower U(IV):mineral ratios. As the U(IV) loading increases, the diminishing availability of surface sites would make adsorption less favorable, so that there is a critical (maximum) coverage above which UO_2 starts to precipitate. With the U(IV) surface complexes identified by X-ray absorption spectroscopy, Latta et al. reported that at pH 7.2 U(IV) could maintain the adsorbed form up to coverages of 1.1 and 0.037 U/nm^2 for rutile and magnetite, respectively.[24] Our modeling results (1.5 and 0.014 U/nm^2) support their observation of the critical coverage for rutile and magnetite (Figure 2a).

Rutile is an extraordinarily strong sorbent for U(IV). At circumneutral pH, it allows up to 70% coverage (calculated from the coverage in U per square nanometer divided by site density in sites per square nanometer) of the total sites without precipitation. Interestingly, stronger adsorption affinity for rutile (as well as anatase) than for iron oxides was also reported for U(VI).[40] Both minerals exhibited a decrease in critical surface coverage with a decrease in pH.

Our models also predict the critical total U(IV) loading that the 2 g/L mineral systems could maintain in the absence of precipitation (Figure 2b). At low pH where U(IV) adsorption was minimal, the critical total U(IV) loading was controlled by UO_2 solubility. Because of their different specific surface areas, the total number of sites on rutile was only $^1/_{10}$ of those on magnetite. However, at circumneutral pH, rutile maintains a system free of UO_2 precipitation with a total U(IV) loading one order of magnitude higher than that of magnetite.

Environmental Implications. Adsorbed U(IV) species may be more common in subsurface environments than previously considered. Under field conditions, the solid-to-water ratios are much higher than in our studies, and there may be more abundant mineral binding sites than those on phosphorus ligands in biomass. Adsorbed U(IV) species may often be overlooked in the microscopic and spectroscopic

characterization of biologically reduced sediments simply because they are very diluted in the solid samples. Gathered by synchrotron spectroscopy, the recent laboratory evidence of surface complexes of U(IV) expanded the diversity of noncrystalline U(IV) species in subsurface processes.[17,22−24] Informed by surface complexation modeling, our results revealed that the adsorption of U(IV) to minerals could maintain dissolved U(IV) concentrations that prevent the supersaturation needed for UO_2 precipitation.

The emerging information about adsorbed U(IV) species requires continuing efforts to characterize their thermodynamic and kinetic properties. Current reactive transport models already incorporate U(VI) surface complexation reactions using laboratory-derived equilibrium and rate constants.[41−44] U(IV) reactions could be included in those models because many aqueous reactions are already available, and this work represents an initial step to establish equilibrium constants for adsorption reactions of U(IV). Built on the studies using model minerals, more realistic simulations can be made in future studies using other media that include amorphous mineral phases, natural organic matter, and biogenic minerals. Mackinawite (FeS), a recently recognized biomass-hosted electron source in microbial uranium reduction,[8] might also be an important adsorbent for U(IV), which could help maintain U(IV) stability.[45] Continued research is warranted to elucidate the mechanisms of coordination of U(IV) to mineral surfaces using various spectroscopic techniques. The fundamental knowledge of adsorption of U(IV) to minerals might allow the development of uranium removal or recovery technologies. The exceptional strength of adsorption of U(IV) to rutile observed recently[24] and in this study, as well the unique U(IV)−Ti bond identified in the U(IV) surface complex on Ti-doped magnetite,[23] all suggested an intriguing role of Ti in controlling the dynamics of U(IV). Brannerite (UTi_2O_6, a common U phase in ores) was found to be more resistant to dissolution than UO_2.[46] Our results also suggested that the formation of the U(IV)−Ti surface complex has a strong thermodynamic favorability.

■ ASSOCIATED CONTENT

Ⓢ Supporting Information

Details of materials and methods, modeling and thermodynamic calculations, additional data for adsorption of U(IV) to hematite, and seven additional figures and three additional tables. The Supporting Information is available free of charge on the ACS Publications website at DOI: 10.1021/acs.estlett.5b00156.

■ AUTHOR INFORMATION

Corresponding Author

*Jerry Yang and Akiko Yamazaki Environment & Energy Building, 473 Via Ortega, Stanford, CA 94305. E-mail: wangzm@stanford.edu. Phone: 650 736-2274.

Notes

The authors declare no competing financial interest.

■ ACKNOWLEDGMENTS

■ REFERENCES

(1) Langmuir, D. Uranium solution-mineral equilibria at low-temperatures with applications to sedimentary ore-deposits. *Geochim. Cosmochim. Acta* **1978**, *42* (6), 547−569.

(2) Singer, D. M.; Chatman, S. M.; Ilton, E. S.; Rosso, K. M.; Banfield, J. F.; Waychunas, G. A. Identification of simultaneous U(VI) sorption complexes and U(IV) nanoprecipitates on the magnetite (111) surface. *Environ. Sci. Technol.* **2012**, *46* (7), 3811−3820.

(3) Latta, D. E.; Boyanov, M. I.; Kemner, K. M.; O'Loughlin, E. J.; Scherer, M. M. Abiotic reduction of uranium by Fe(II) in soil. *Appl. Geochem.* **2012**, *27* (8), 1512−1524.

(4) Latta, D. E.; Gorski, C. A.; Boyanov, M. I.; O'Loughlin, E. J.; Kemner, K. M.; Scherer, M. M. Influence of magnetite stoichiometry on U^{VI} reduction. *Environ. Sci. Technol.* **2012**, *46* (2), 778−786.

(5) Hua, B.; Xu, H.; Terry, J.; Deng, B. Kinetics of uranium (VI) reduction by hydrogen sulfide in anoxic aqueous systems. *Environ. Sci. Technol.* **2006**, *40* (15), 4666−4671.

(6) Lovley, D. R.; Phillips, E. J. P.; Gorby, Y. A.; Landa, E. R. Microbial reduction of uranium. *Nature* **1991**, *350* (6317), 413−416.

(7) Williams, K. H.; Bargar, J. R.; Lloyd, J. R.; Lovley, D. R. Bioremediation of uranium-contaminated groundwater: a systems approach to subsurface biogeochemistry. *Curr. Opin. Biotechnol.* **2013**, *24* (3), 489−497.

(8) Bargar, J. R.; Williams, K. H.; Campbell, K. M.; Long, P. E.; Stubbs, J. E.; Suvorova, E. I.; Lezama-Pacheco, J. S.; Alessi, D. S.; Stylo, M.; Webb, S. M.; Davis, J. A.; Giammar, D. E.; Blue, L. Y.; Bernier-Latmani, R. Uranium redox transition pathways in acetate-amended sediments. *Proc. Natl. Acad. Sci. U. S. A.* **2013**, *110* (12), 4506−4511.

(9) Bargar, J. R.; Bernier-Latmani, R.; Giammar, D. E.; Tebo, B. M. Biogenic uraninite nanoparticles and their importance for uranium remediation. *Elements* **2008**, *4* (6), 407−412.

(10) Burgos, W. D.; McDonough, J. T.; Senko, J. M.; Zhang, G. X.; Dohnalkova, A. C.; Kelly, S. D.; Gorby, Y.; Kemner, K. M. Characterization of uraninite nanoparticles produced by Shewanella oneidensis MR-1. *Geochim. Cosmochim. Acta* **2008**, *72* (20), 4901−4915.

(11) Hyun, S. P.; Davis, J. A.; Sun, K.; Hayes, K. F. Uranium(VI) reduction by iron(II) monosulfide mackinawite. *Environ. Sci. Technol.* **2012**, *46* (6), 3369−3376.

(12) Bernier-Latmani, R.; Veeramani, H.; Vecchia, E. D.; Junier, P.; Lezama-Pacheco, J. S.; Suvorova, E. I.; Sharp, J. O.; Wigginton, N. S.; Bargar, J. R. Non-uraninite products of microbial U(VI) reduction. *Environ. Sci. Technol.* **2010**, *44* (24), 9456−9462.

(13) Fletcher, K. E.; Boyanov, M. I.; Thomas, S. H.; Wu, Q. Z.; Kemner, K. M.; Loffler, F. E. U(VI) reduction to mononuclear U(IV) by *Desulfitobacterium* species. *Environ. Sci. Technol.* **2010**, *44* (12), 4705−4709.

(14) Sharp, J. O.; Lezama-Pacheco, J. S.; Schofield, E. J.; Junier, P.; Ulrich, K. U.; Chinni, S.; Veeramani, H.; Margot-Roquier, C.; Webb, S. M.; Tebo, B. M.; Giammar, D. E.; Bargar, J. R.; Bernier-Latmani, R. Uranium speciation and stability after reductive immobilization in aquifer sediments. *Geochim. Cosmochim. Acta* **2011**, *75* (21), 6497−6510.

(15) Kelly, S. D.; Wu, W.-M.; Yang, F.; Criddle, C. S.; Marsh, T. L.; O'Loughlin, E. J.; Ravel, B.; Watson, D.; Jardine, P. M.; Kemner, K. M. Uranium transformations in static microcosms. *Environ. Sci. Technol.* **2010**, *44* (1), 236−242.

(16) Alessi, D. S.; Lezama-Pacheco, J. S.; Stubbs, J. E.; Janousch, M.; Bargar, J. R.; Persson, P.; Bernier-Latmani, R. The product of microbial uranium reduction includes multiple species with U(IV)-phosphate coordination. *Geochim. Cosmochim. Acta* **2014**, *131*, 115−127.

(17) Boyanov, M. I.; Fletcher, K. E.; Kwon, M. J.; Rui, X.; O'Loughlin, E. J.; Loffler, F. E.; Kemner, K. M. Solution and microbial controls on the formation of reduced U(IV) species. *Environ. Sci. Technol.* **2011**, *45* (19), 8336−8344.

(18) Cerrato, J. M.; Ashner, M. N.; Alessi, D. S.; Lezama Pacheco, J. S.; Bernier-Latmani, R.; Bargar, J.; Giammar, D. E. Relative reactivity of biogenic and chemogenic uraninite and biogenic non-crystalline U(IV). *Environ. Sci. Technol.* **2013**, *47* (17), 9756−9763.

(19) Alessi, D. S.; Uster, B.; Veeramani, H.; Suvorova, E. I.; Lezama-Pacheco, J. S.; Stubbs, J. E.; Bargar, J. R.; Bernier-Latmani, R. Quantitative separation of monomeric U(IV) from UO$_2$ in products of U(VI) reduction. *Environ. Sci. Technol.* **2012**, *46* (11), 6150−6157.

(20) Stylo, M.; Alessi, D. S.; Shao, P. P.; Lezama-Pacheco, J. S.; Bargar, J. R.; Bernier-Latmani, R. Biogeochemical controls on the product of microbial U(VI) reduction. *Environ. Sci. Technol.* **2013**, *47* (21), 12351−12358.

(21) Veeramani, H.; Scheinost, A. C.; Monsegue, N.; Qafoku, N. P.; Kukkadapu, R.; Newville, M.; Lanzirotti, A.; Pruden, A.; Murayama, M.; Hochella, M. F. Abiotic reductive immobilization of U(VI) by biogenic mackinawite. *Environ. Sci. Technol.* **2013**, *47* (5), 2361−2369.

(22) Chakraborty, S.; Favre, F.; Banerjee, D.; Scheinost, A. C.; Mullet, M.; Ehrhardt, J.-J.; Brendle, J.; Vidal, L. c.; Charlet, L. U(VI) sorption and reduction by Fe(II) sorbed on montmorillonite. *Environ. Sci. Technol.* **2010**, *44* (10), 3779−3785.

(23) Latta, D. E.; Pearce, C. I.; Rosso, K. M.; Kemner, K. M.; Boyanov, M. I. Reaction of U^{VI} with titanium-substituted magnetite: Influence of Ti on U^{IV} speciation. *Environ. Sci. Technol.* **2013**, *47* (9), 4121−4130.

(24) Latta, D. E.; Mishra, B.; Cook, R. E.; Kemner, K. M.; Boyanov, M. I. Stable U(IV) complexes form at high-affinity mineral surface sites. *Environ. Sci. Technol.* **2014**, *48* (3), 1683−1691.

(25) Veeramani, H.; Alessi, D. S.; Suvorova, E. I.; Lezama-Pacheco, J. S.; Stubbs, J. E.; Sharp, J. O.; Dippon, U.; Kappler, A.; Bargar, J. R.; Bernier-Latmani, R. Products of abiotic U(VI) reduction by biogenic magnetite and vivianite. *Geochim. Cosmochim. Acta* **2011**, *75* (9), 2512−2528.

(26) Scott, T. B.; Allen, G. C.; Heard, P. J.; Randell, M. G. Reduction of U(VI) to U(IV) on the surface of magnetite. *Geochim. Cosmochim. Acta* **2005**, *69* (24), 5639−5646.

(27) Ilton, E. S.; Boily, J.-F.; Buck, E. C.; Skomurski, F. N.; Rosso, K. M.; Cahill, C. L.; Bargar, J. R.; Felmy, A. R. Influence of dynamical

conditions on the reduction of U^{VI} at the magnetite–solution interface. *Environ. Sci. Technol.* **2010**, *44* (1), 170−176.

(28) Skomurski, F. N.; Ilton, E. S.; Engelhard, M. H.; Arey, B. W.; Rosso, K. M. Heterogeneous reduction of U^{6+} by structural Fe^{2+} from theory and experiment. *Geochim. Cosmochim. Acta* **2011**, *75* (22), 7277−7290.

(29) Missana, T.; Garcia-Gutierrez, M.; Fernndez, V. Uranium(VI) sorption on colloidal magnetite under anoxic environment: Experimental study and surface complexation modelling. *Geochim. Cosmochim. Acta* **2003**, *67* (14), 2543−2550.

(30) Missana, T.; Maffiotte, U.; Garcia-Gutierrez, M. Surface reactions kinetics between nanocrystalline magnetite and uranyl. *J. Colloid Interface Sci.* **2003**, *261* (1), 154−160.

(31) Wang, Z.; Lee, S.-W.; Kapoor, P.; Tebo, B. M.; Giammar, D. E. Uraninite oxidation and dissolution induced by manganese oxide: A redox reaction between two insoluble minerals. *Geochim. Cosmochim. Acta* **2013**, *100* (1), 24−40.

(32) Schecher, W. D.; McAvoy, D. C. *MINEQL+: A chemical equilibrium modeling system*, version 4.6; Environmental Research Software: Hallowell, ME, 2007.

(33) Wang, Z.; Giammar, D. E. Mass action expressions for bidentate adsorption in surface complexation modeling: Theory and practice. *Environ. Sci. Technol.* **2013**, *47* (9), 3982−3996.

(34) Sverjensky, D. A. Standard states for the activities of mineral surface sites and species. *Geochim. Cosmochim. Acta* **2003**, *67* (1), 17−28.

(35) Davis, J. A.; Kent, D. B. Surface complexation modeling in aqueous geochemistry. *Rev. Mineral. Geochem.* **1990**, *23* (1), 177−260.

(36) Eichholz, G.; Nagel, A. E.; Hughes, R. Adsorption of ions dilute aqueous solutions on glass and plastic surfaces. *Anal. Chem.* **1965**, *37* (7), 863−868.

(37) Struempler, A. W. Adsorption characteristics of silver, lead, cadmium, zinc, and nickel on borosilicate glass, polyethylene, and polypropylene container surfaces. *Anal. Chem.* **1973**, *45* (13), 2251−2254.

(38) Guillaumont, R.; Fanghänel, T.; Fuger, J.; Grenthe, I.; Neck, V.; Palmer, D. A.; Rand, M. H. *Update on the Chemical Thermodynamics of Uranium, Neptunium, Plutonium, Americium and Technetium*; Elsevier: Washington, DC, 2003.

(39) Opel, K.; Weiss, S.; Hübener, S.; Zänker, H.; Bernhard, G. Study of the solubility of amorphous and crystalline uranium dioxide by combined spectroscopic methods. *Radiochim. Acta* **2007**, *95* (3), 143−149.

(40) Payne, T.; Lumpkin, G.; Waite, T. Uranium (VI) adsorption on model minerals. In *Adsorption of Metals by Geomedia*; Jenne, E. A., Ed.; Academic Press: San Diego, 1998; pp 75−97.

(41) Kohler, M.; Curtis, G. P.; Kent, D. B.; Davis, J. A. Experimental investigation and modeling of uranium(VI) transport under variable chemical conditions. *Water Resour. Res.* **1996**, *32* (12), 3539−3551.

(42) Miller, A. W.; Rodriguez, D. R.; Honeyman, B. D. Upscaling sorption/desorption processes in reactive transport models to describe metal/radionuclide transport: A critical review. *Environ. Sci. Technol.* **2010**, *44* (21), 7996−8007.

(43) Dong, W.; Wan, J. Additive surface complexation modeling of uranium(VI) adsorption onto quartz-sand dominated sediments. *Environ. Sci. Technol.* **2014**, *48* (12), 6569−6577.

(44) Wang, Z.; Lee, S.-W.; Catalano, J. G.; Lezama-Pacheco, J. S.; Bargar, J. R.; Tebo, B. M.; Giammar, D. E. Adsorption of uranium(VI) to manganese oxides: X-ray absorption spectroscopy and surface complexation modeling. *Environ. Sci. Technol.* **2013**, *47* (2), 850−858.

(45) Bi, Y.; Hayes, K. F. Nano-FeS inhibits UO$_2$ reoxidation under varied oxic conditions. *Environ. Sci. Technol.* **2014**, *48* (1), 632−640.

(46) Zhang, Y.; Thomas, B. S.; Lumpkin, G. R.; Blackford, M.; Zhang, Z.; Colella, M.; Aly, Z. Dissolution of synthetic brannerite in acidic and alkaline fluids. *J. Nucl. Mater.* **2003**, *321* (1), 1−7.

(47) Pabalan, R.; Turner, D.; Bertetti, F.; Prikryl, J. Uranium (VI) sorption onto selected mineral surfaces: Key geochemical parameters. In *Adsorption of metals by geomedia: Variables, mechanisms, and model applications*; Jenne, E. A., Ed.; Academic Press: San Diego, 1998; pp 99−130.

(48) Dixit, S.; Hering, J. G. Comparison of arsenic(V) and arsenic(III) sorption onto iron oxide minerals: Implications for arsenic mobility. *Environ. Sci. Technol.* **2003**, *37* (18), 4182−4189.

(49) Wang, X.; Shi, K.; Guo, Z.; Wu, W. Eu (III) adsorption on rutile: Batch experiments and modeling. *Sci. China: Chem.* **2010**, *53* (12), 2628−2636.

(50) Milonjić, S.; Bošković, M.; Ćeranić, T. Adsorption of uranium (VI) and zirconium (IV) from acid solutions on silica gel. *Sep. Sci. Technol.* **1992**, *27* (12), 1643−1653.

(51) Lu, S.; Guo, Z.; Zhang, C.; Zhang, S. Sorption of Th (IV) on MX-80 bentonite: effect of pH and modeling. *J. Radioanal. Nucl. Chem.* **2011**, *287* (2), 621−628.